Holographic investigation of $Pb_{0.9}La_{0.1}(Zr_{0.65}Ti_{0.35})_{0.975}O_3$ ceramics close to the diffuse phase transition

Romano A. Rupp
Fachbereich Physik, Universität Osnabrück, D-4500 Osnabrück, Federal Republic of Germany

Andris E. Krumins
Institute of Solid State Physics of the Latvian State University, 226063 Riga, U.S.S.R.

Karl Kerperin and Ralph Matull
Fachbereich Physik, Universität Osnabrück, D-4500 Osnabrück, Federal Republic of Germany
(Received 18 July 1988; revised manuscript received 4 October 1988)

Holographic gratings are recorded in $Pb_{0.9}La_{0.1}(Zr_{0.65}Ti_{0.35})_{0.975}O_3$ (PLZT 10:65:35) samples. The first and second Fourier order of the refractive index amplitude, its phase shift against the periodic light intensity pattern, and the holographic gain are measured as a function of exposure, grating spacing, and the electric fields applied during writing and reading. The data are analyzed by a phenomenological theory which allows for bipolar conductivity with nonproportional dependence on the light intensity and light scattering and a nonlinear dependence of the dielectric and electro-optic properties on the applied electric field due to the diffuse phase transition of PLZT 10:65:35. The second-order diffraction efficiency is an asymmetrical function of the reading field and possesses a minimum. Second-order diffraction is the basis of a new holographic method for the measurement of the absolute value of the electro-optic coefficient. The conductivity modulation factor κ can be determined from gain measurements. Hysteretic behavior of the refractive index amplitudes and inhomogeneously distributed regions with remanent first-order diffraction can be attributed to polar microregions.

I. INTRODUCTION

In photorefractive materials holographic recording is due to a light-induced charge transport. Electrons or holes are released from filled donor or acceptor centers upon photoexcitation and migrate by virtue of diffusion, drift or photovoltaic effect until they are caught by empty donor (acceptor) centers at sites different from the points of departure. The resulting space charge density modulates the electric displacement field or the electric polarization, respectively, and via the electrooptic effect also the refractive index. A well established method for the investigation of the charge transport is the holographic method, where a periodically modulated light intensity with fringe spacing Λ is used for the investigation.

One of the key parameters for the characterization of photorefractive materials is E_q. Roughly speaking, E_q defines the maximum space charge field amplitude which can be achieved in a photorefractive process by infinitely large diffusion, photovoltaic or externally applied electric driving fields, if quantities involved in the photorefractive effect are constrained to be sinusoidally modulated with grating spacing Λ. The space charge density amplitude which can be achieved is limited by the available average density of filled or empty donors or acceptors (whichever is smaller). Because a fraction of the space charge density has to balance the (bound) polarization charges, the effectiveness of the charge density amplitude for the build up of an electric field decreases with increasing polarizability. For a given space charge density amplitude the pertinent space charge field decreases with increasing spatial frequency $K=2\pi/\Lambda$. Hence E_q increases with the density of filled and empty donors (acceptors) and is inversely proportional to the permittivity and K (limiting the resolution of the material).

For $LiNbO_3$ and $LiTaO_3$ there are no apparent limitations for the space charge field amplitude by K, for these materials have low permittivity and are usually doped so that E_q is extremely large. The space charge field is confined by the driving fields of the involved charge transport processes which may be characterized by the so-called diffusion field E_D, the so-called photovoltaic field E_{ph}, and the externally applied electric field E_{ex}. The stationary energy transfer between the recording beams in large external or photovoltaic fields is small, because the phase mismatch ϕ_g between the holographic grating and the fringe pattern decreases with $E_{ex}+E_{ph}$.[1-3]

In materials with large photoconductivity the restriction of the space charge field, however, plays an important role despite a relatively small dielectric constant. This is the case for $KNbO_3$, $Bi_{12}GeO_{20}$, and $Bi_{12}SiO_{20}$ (Table I). The large photoconductivity is caused by a large drift length $L_E=\mu\tau E_{ex}$ which is comparable to the grating spacing (violation of quasineutrality).[1,3-5] This causes a stationary energy transfer between the recording beams characterized by the value of the exponential gain Γ which increases with E_{ex}.

TABLE I. Specific photoconductivity ($\Phi\mu\tau$), relative dielectric constant (ϵ), acceptor density N_A, and maximum space charge fields E_q of some electrooptic materials at grating spacing $\Lambda = 1\,\mu$m.

Material	$\Phi\mu\tau$ ($m^2 V^{-1}$)	ϵ	N_A (10^6 m^{-3})	E_q (10^5 $V m^{-1}$)	Ref.
$KNbO_3$	0.19×10^{-7}	50	10^{15}	7	3
$Bi_{12}SiO_{20}$	1.0×10^{-7}	56	10^{15}	7	4
$Bi_{12}GeO_{20}$	0.84×10^{-7}	60	6×10^{15}	2.1	5
PLZT	1.0×10^{-11}	4500	10^{18}	10	7

In $(Pb_{0.9}La_{0.1}(Zr_{0.65}Ti_{0.35})_{0.975}O_3)$ (PLZT 10:65:35) ceramics the defect concentration is large and, as a consequence, the drift length usually smaller than the grating spacing.[7] Therefore the photoconductivity is small (Table I). Nevertheless experiments substantiate that the exponential gain is larger than in the other mentioned crystals.[8] Energy transfer and diffraction efficiency as functions of the grating spacing and the applied field can be described by the dynamic theory[9] assuming that quasineutrality does not hold.[8]

In the room temperature phase diagram[10] the compositions PLZT 8–10:65:35 are located very close to the cross over of four different phases, namely the ferroelectric rhombohedral and the paraelectric cubic phase along increasing La concentration and the ferroelectric tetragonal and the antiferroelectric orthorhombic[11] phase along increasing [Zr]/[Ti] ratio. (We disregard here the antiferroelectric tetragonal phase suggested by Kumada *et al.*,[12] because the experimental evidence is not convincing.) Because of this exceptional position it can be expected that the material will be highly sensitive to small changes of external parameters. As a consequence PLZT 10:65:35 has a large static dielectric constant ϵ at room temperature (Table II). This makes PLZT 10:65:35 an excellent choice for the holographic investigation of space charge limited fields. In this article we present results on the phase mismatch between the periodic light intensity pattern and the refractive index grating as a function of the electric writing field and determine the important material parameter E_q. We will prove that it is possible to exceed E_q already with moderate electric fields.

In the holographic literature the compositions PLZT X:65:35 with $x > 9$ are usually regarded as simple nonpolar quadratic materials.[8,13–15] Because of the diffuse phase transition this is strictly speaking not correct and some other authors[7,16–20] are well aware of this fact but do not draw any consequences of it. Among the peculiarities which are important for holographic investigations are nonlinear dielectric properties which lead to an electrooptic response which is not quadratic in the applied electric field but involves at least fourth-order contributions.[21] Therefore our data are analyzed by a phenomenologic theory of the photorefractive effect which takes into account to a certain extent the nonlinear dielectric properties, a nonlinear relationship between conductivity and light intensity and bipolar conductivity. Furthermore, we strictly utilize the space charge polarization concept instead of a space charge field concept and take advantage of the polarization electrooptic effect which remains in contrast to the electric field induced electrooptic effect quadratic.

The first- and second-order Fourier components of the recorded refractive index amplitude are studied as a function of the reading and the writing field. It has not been realized up to now that the second-order Fourier component gives us an easy access to interesting material parameters. The holographic gain Γ is measured as a function of the external electric field and of the grating period Λ.

II. PHENOMENOLOGIC THEORY OF THE PHOTOREFRACTIVE PROCESS

In order to bring out the main issues of our considerations more clearly we use the following simplification justified by our experiments:

(1) The ceramic is periodically illuminated in a two-beam interference set up (Fig. 1). The grating vector **K** and an eventually applied electric field are parallel to the z axis. Vector quantities which occur in the charge transport equations are directed parallel to the z axis. All quantities depend periodically on the z coordinate. The dependence on the y coordinate is weak and enters the transport equations merely as a parameter. We will suppress therefore the y coordinate in the argument of all field quantities and treat for a given y value a one-dimensional model. If there is no light scattering or absorption, the periodic light modulation is given by

$$I(z) = I_0[1 + M(z)] = I_0[1 + m\cos(Kz)]\,, \tag{1a}$$

TABLE II. Static dielectric constant ϵ for PLZT 10:65:35.

ϵ (10^3)	ν (Hz)	T (°C)	Condition	Ref.
4.0	10^3	25	aged	44
4.5	0.1	25	thermally depoled	45
4.8	10^3	25	thermally depoled	44
5.05		room temperature		36
8.0		25		46

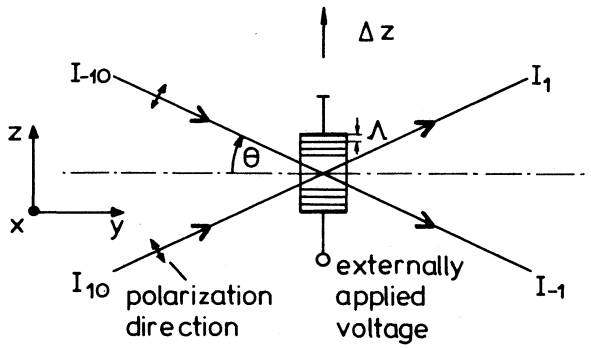

FIG. 1. Sketch of the coordinate system and the experimental setup for holographic recording and measurements of the gain Γ. For determination of the phase mismatch $\phi_g(K)$ the sample which is mounted on a translation table is shifted along the z-axis by a piezoelectric transducer. The shift by an amount Δz corresponds to an external phase shift $\psi=2\pi\Delta z/\Lambda$. The diffraction efficiency η_{+1} is measured with the beam intensity I_{+10} blocked off and η_{-1} vice versa.

where $I_0=I_{+1}+I_{-1}$ is the average intensity, $M(z)$ the modulated portion and $m=2\sqrt{I_{+1}I_{-1}}/I_0$ the modulation degree. For simplicity of notation we have omitted a phase shift ϕ_I depending on the y coordinate. If the dynamic read-write process is explicitly considered, we have to remember that this additional phase shift must be included for all periodic functions which follow.

(2) In case of absorption I_0 decays with y. This obviously influences the dynamics. But as m remains unchanged, absorption will be disregarded here, because we intend to consider only the stationary state in the following. Effects due to a modulated absorption constant are discussed later.

(3) If the two writing beams and (elastically or quasielastically) scattered light beams interact, a rather complex interference pattern may result. We will assume here that the intensity scattered into some arbitrary direction is small compared to the intensities I_{+1} and I_{-1} of the two writing beams, but that the integral (sum) of the intensities scattered into all directions may be large. Three contributions in the Fourier transformed intensity pattern of some plane $y=$const can be classified according to their spatial frequency: (i) The intensity Fourier component with spatial frequency 0 is the integral of all beams, i.e., is equal to $I_{+1}+I_{-1}+I_s$, where I_s is the integral (sum) of all the scattered beam intensities. (ii) The Fourier component with spatial frequency K is mainly due to the writing beams. Besides their intensity Fourier component $2\sqrt{I_{+1}I_{-1}}$, other contributions with spatial frequency K are negligible. (iii) All other spatial frequencies are generated by the interaction of the scattered beams with each other or with one of the writing beams. Their intensity Fourier component is proportional to the square root of the product of their intensities. As we have assumed small scattered intensities in a particular direction, the pertinent Fourier component of the intensity pattern is small compared to the first mentioned contributions, i.e., also the pertinent light intensity modulation is negligibly small. Furthermore, we investigate only contributions with 0, K and 2 K experimentally. Thus in the lowest approximation scattered light acts in our case merely as a light background and is taken into account by

$$I(z)=I_0[1+M(z)]+I_s=I_0[1+m\cos(Kz)]+I_s\ , \tag{1b}$$

where I_0, $M(z)$ and m refer to the two writing beams as defined above. For volume scattering it is understood that I_0 decays exponentially with y and I_s increases correspondingly.[34]

(4) Only the stationary state is treated, i.e., all time derivatives are zero. We proceed from the basic equation system:

$$\nabla D(z)=\rho(z)\ , \tag{2}$$

$$\nabla j(z)=0\ , \tag{3}$$

where ∇ denotes the derivative with respect to z, $D(z)$ the dielectric displacement, $\rho(z)$ the space charge density, and

$$j(z)=[\sigma_p(z)+\sigma_n(z)]E(z)+\frac{k_BT}{e}\nabla[\sigma_n(z)-\sigma_p(z)] \tag{4}$$

the current density. Here $\sigma_p(z)$ and $\sigma_n(z)$ are the partial conductivities for p-type (positive) and n-type (negative) charge carriers, respectively, $E(z)$ is the electric field, k_BT the thermal energy, and e the unit charge. We have used the Einstein relation, we assume that the mobility is not spatially modulated and take notice of the experimental result that the photovoltaic contribution does not play any role for PLZT 10:65:35.[22]

(5) The photoconductivity σ_{ph} of PLZT for a constant illumination with intensity I_0 is either of n-type,[14,15] p-type,[8,13,23] or both contributions nearly balance each other[19] (so-called compensated bipolar conductivity). The electronic[24] or ionic[25] dark conductivity σ_d is usually neglected in the evaluation of holographic experiments.[14,15,19] Using the values $\sigma_d=3\times10^{-13}\ \Omega^{-1}\,\mathrm{m}^{-1}$ and $\sigma_{ph}/I_0=8\times10^{-14}\ \Omega^{-1}\,\mathrm{W}^{-1}\,\mathrm{m}$ of PLZT 9:65:35,[13] we have $\sigma_d/\sigma_{ph}\approx4\%$ for $I_0=10^2\,\mathrm{W\,m}^{-2}$ (the order of magnitude used in our experiments). As no data for PLZT 10:65:35 are available to us we are not sure that dark conductivity contributions can be neglected. They will therefore be retained in our analysis. Holographic theories are based on the assumption that the photoconductivity is proportional to the light intensity, while a sublinear relationship $\sigma_{ph}=AI_0^x$ with $0.5\le x\le1$ and a constant of proportionality A has been proven experimentally.[26] As the discussion of the microscopic origin of the charge transport mechanism is still not settled, we postulate that the expressions

$$\sigma_p(z)=\tfrac{1}{2}\sigma_0(1-\hat{\sigma})[1+\kappa_pM(z)+\rho(z)/eN_p]\ , \tag{5a}$$

$$\sigma_n(z)=\tfrac{1}{2}\sigma_0(1+\hat{\sigma})[1+\kappa_nM(z)-\rho(z)/eN_n]\ , \tag{5b}$$

hold for the partial conductivities [which are naturally not observed separately but enter Eq. (4) as sum and difference]. Here $\sigma_0=\sigma_d+\sigma_{ph}$ is the total conductivity for constant total average illumination with intensity I_0+I_s, and $\hat{\sigma}$ the conductivity type factor as defined in Ref. 27. Its values range from $\hat{\sigma}=-1$ for pure p-type conductivity over $\hat{\sigma}=0$ for exactly compensated bipolar conductivity to $\hat{\sigma}=1$ for the case of pure n-type conductivity. The phenomenologic constants κ_p and κ_n take the possibility into account that the partial conductivities are not directly proportional to the light intensity. The phenomenologic constants eN_p and eN_n ensure that the space charge field amplitude is limited by the finite density of photoactive flaw centers. The latter effect has been revealed recently to be the most important effect for the development process of thermally fixed gratings.[28]

In order to illustrate the meaning of κ_p and κ_n let us consider the limiting case $\hat{\sigma}=-1$ of dominating hole conductivity and neglect $\rho(z)/eN_p$ (possible for $N_p\to\infty$ or $K\to 0$). Then $\sigma(z)=\sigma_d+A(I(z))^x$. Using Eq. (1b) in the small modulation approximation we get

$$\sigma(z)\approx(\sigma_d+\sigma_{ph})[1+x(1+I_s/I_0)^{-1}\times(1+\sigma_d/\sigma_{ph})^{-1}M(z)]\ ,$$

where $\sigma_{ph}=A(I_0+I_s)^x$ is the average (unmodulated) photoconductivity and we easily identify

$$\kappa_p\approx x_p(1+I_s/I_0)^{-1}(1+\sigma_d/\sigma_{ph})^{-1}\ ,$$

where x_p is the exponent for p-type photoconductivity. The effective conductivity modulation factors κ_p and κ_n are smaller than 1 due to three possible reasons, (i) a sublinear dependence of the photoconductivity on the light intensity, (ii) dark conductivity, and (iii) light scattering. The values for x are expected to be between $\frac{1}{2}$ and 1, i.e., the difference is not large. Then a detailed calculation shows for $\kappa_p\neq\kappa_n$ that only some corrections of minor importance result only for the case of nearly compensated bipolar conductivity. We feel that it is not justified to present the resulting elaborate formula to the reader and assume in the following that $\kappa_p\approx\kappa_n=\kappa$ which simplifies our results considerably.

(6) The fundamental fields $E(z)$, $\rho(z)$, and $I(z)$ are nonlinearly related via the material quantities $j(z)$ and $D(z)$. But all fields are periodic with fundamental spatial frequency K. We are interested in effects of first and second order and truncate adequately all Fourier series which appear in our calculation. For the convolution only the largest terms are taken into account. Two examples will show how we proceed and which notation we use:

$$E(z)\approx E(0)+\tfrac{1}{2}[E(K)e^{iKz}+E(2K)e^{2iKz}+\text{c.c.}]\ , \tag{6}$$

$$\nabla(\sigma(z)E(z))\approx\tfrac{1}{2}iK[\sigma(0)E(K)+\sigma(K)E(0)]e^{iKz}+iK[\sigma(2K)E(0)+\tfrac{1}{2}\sigma(K)E(K)+\sigma(0)E(2K)]e^{2iKz}+\text{c.c.}\ . \tag{7}$$

Here $E(0)$ and $\sigma(0)$ denote the Fourier coefficients $E(K=0)$ and $\sigma(K=0)$ and "c.c." the complex conjugate expressions. The solution for the first-order Fourier component only is popularly called the small modulation approximation. Its validity is discussed e.g., by Hall *et al.*[29] It is necessary for materials with quadratic electrooptic effect to consider also the second order Fourier component in order to explain some surprising results observed by diffraction experiments at the second order Bragg angle.

(7) An electric field E_W which is applied to a sample with platelike geometry at the beginning of holographic writing induces a constant polarization P_W as long as the sample is still free of space charges. After recording the sample has the periodically modulated polarization $P(z)$. Unfortunately there is no linear relationship between polarization and electric field for PLZT 10:65:35 because the room temperature range is affected by a diffuse phase transition.[21] But we can take advantage of the fact that the nonlinearity is small for PLZT 10:65:35 which allows the approximation

$$E(P(z))\approx E(P_W)+\left[\frac{\partial E}{\partial P}\right]_{P_W}[P(z)-P_W]\ . \tag{8}$$

The nonlinearity enters to a first approximation only via the field dependent susceptibility $\epsilon_0\chi(E_W)=1/(\partial E/\partial P)_{P_W}$, where ϵ_0 denotes the vacuum permittivity.

The Fourier series of the fields and the approximated expression for the convolution are inserted into the Fourier transformed Eqs. (2)–(5) and rearranged according to equal powers of $\exp(iKz)$. The first order solution of the polarization amplitude is given by:

$$P(K)=-\kappa m\epsilon_0\chi(E_W)\frac{E_W+i\hat{\sigma}E_D}{1+E_D/E_{qd}-iE_W/E_{qe}}\ . \tag{9}$$

Here $E_D=Kk_BT/e$ is the diffusion field,

$$E_{qd}=\left[\epsilon_0\epsilon(E_W)K\left[\frac{1+\hat{\sigma}}{2eN_n}+\frac{1-\hat{\sigma}}{2eN_p}\right]\right]^{-1} \tag{10a}$$

and

$$E_{qe}=\left[\epsilon_0\epsilon(E_W)K\left[\frac{1+\hat{\sigma}}{2eN_n}-\frac{1-\hat{\sigma}}{2eN_p}\right]\right]^{-1} \tag{10b}$$

are the maximum space charge field amplitudes, and $\epsilon(E_W)=1+\chi(E_W)$ is the field dependent relative permittivity.

For the second-order solution we obtain

$$P(2K)=-\tfrac{1}{2}\kappa mP(K)\frac{1+\dfrac{E_D}{E_{qd}}-\hat{\sigma}\dfrac{E_D}{E_{qe}}}{(1+4E_D/E_{qd}-2iE_W/E_{qe})(1+E_D/E_{qd}-iE_W/E_{qe})}\ . \tag{11}$$

In Eq. (11) we have terms with e.g., $2E_D/E_{qd}$ instead of E_D/E_{qd} in the denominator of Eq. (9) because for the second-order K has to be replaced by $2K$, E_D by $2E_D$, E_{qd} by $E_{qd}/2$, and E_{qe} by $E_{qe}/2$.

If the electrooptic effect of PLZT 10:65:35 is expressed by electric fields, the relationship is rather complex because of the influence of the diffuse phase transition and e.g., fourth-order contribution are involved.[21] This complication can be avoided by choosing a description in terms of polarization. Then the electrooptic index change is still a simple quadratic function of the polarization in the quasiparaelectric range of the diffuse phase transition:

$$\Delta n_\alpha(z) = -\tfrac{1}{2}n^3 g_{\alpha 3} P^2(z) = -\tfrac{1}{2}n^3 g_{\alpha 3}\{P_R^2 + \tfrac{1}{2}P_{SC}^2(K) + 2P_R P_{SC}(K)\cos[Kz+\phi_g(K)] + \tfrac{1}{2}P_{SC}^2(K) f(E_R)\cos[2Kz+\phi_g(2K)] + \cdots\} . \tag{12}$$

In Eq. (12) only terms up to the second order of the Fourier series are considered, terms which are larger than quadratic powers of κm are neglected, Δn_α denotes the modulated refractive index change, n the average refractive index, $g_{\alpha 3}$ the quadratic electrooptic coefficient ($\alpha = 1, \ldots, 6$, Voigt's notation) for polarization fields, and $P_R = P(E_R) \approx \epsilon_0 \chi(E_R) E_R$ the unmodulated portion of the polarization induced by applying an electric field E_R during read out (which may be different from the field E_W applied during writing of the hologram). The magnitude of the space charge polarization amplitude is given by

$$P_{SC}(K) = |P(K)| = \kappa m \epsilon_0 \chi(E_W) \frac{\left[\left[E_W + E_W\frac{E_D}{E_{qd}} - E_W\hat{\sigma}\frac{E_D}{E_{qd}}\right]^2 + \left[\hat{\sigma}E_D + \hat{\sigma}\frac{E_D^2}{E_{qd}} + \frac{E_W^2}{E_{qe}}\right]^2\right]^{1/2}}{(1+E_D/E_{qd})^2 + (E_W/E_{qe})^2} \tag{13}$$

and the stationary phase shift $\phi_g(K)$ between the fundamental component of the pertinent refractive index grating and the light intensity pattern by

$$\tan\phi_g(K) = \frac{\hat{\sigma}\frac{E_D}{E_W} + \frac{E_W}{E_{qe}} + \hat{\sigma}\frac{E_D^2}{E_W E_{qd}}}{1 + E_D/E_{qd} - \hat{\sigma}E_D/E_{qe}} . \tag{14}$$

The second-order Fourier component is characterized by the function

$$f(E_R) = \left[\left[1 + 2\frac{\zeta_1}{\zeta_3}\frac{E_W E_R}{E_W^2 + (\hat{\sigma}E_D)^2}\right]^2 + \left[2\frac{\zeta_2}{\zeta_3}\frac{\hat{\sigma}E_D E_R}{E_W^2 + (\hat{\sigma}E_D)^2}\right]^2\right]^{1/2} , \tag{15a}$$

and the pertinent phase shift by

$$\phi_g(2K) = 2\phi_g(K) - \arctan\frac{2\zeta_2\hat{\sigma}E_D E_R}{\zeta_3[E_W^2 + (\hat{\sigma}E_D)^2] + 2\zeta_1 E_W E_R} . \tag{15b}$$

Above we have used the abbreviations

$$\zeta_1 = (1 + E_D/E_{qd} - \hat{\sigma}E_D/E_{qe}) \times (1 + 4E_D/E_{qd} + 2\hat{\sigma}E_D/E_{qe}) ,$$

$$\zeta_2 = (1 + E_D/E_{qd} - \hat{\sigma}E_D/E_{qe}) \times (1 + 4E_D/E_{qd} - 2E_W^2/\hat{\sigma}E_D E_{qe}) ,$$

and

$$\zeta_3 = (1 + 4E_D/E_{qd})^2 + (2E_W/E_{qe})^2 .$$

The diffraction efficiencies η_1 at the first order Bragg angle θ_1 and η_2 at the second-order Bragg angle θ_2 are given by[30]

$$\eta_{1,2} = \sin^2(\pi\Delta n_{1,2} d/\lambda\cos\theta'_{1,2}) , \tag{16}$$

where the primes mark quantities measured within the sample, d is the thickness of the sample, λ is the wavelength of the light,

$$\Delta n_1 = n^3 g_{\text{eff}} P_R P_{SC}(K) , \tag{17a}$$

$$\Delta n_2 = \tfrac{1}{4}n^3 g_{\text{eff}} P_{SC}^2(K) f(E_R) , \tag{17b}$$

$g_{\text{eff}} = g_{13}\sin^2\phi + [g_{33}\cos^2\theta_m - g_{13}\sin^2\theta_m]\cos^2\phi$, and ϕ denotes the angle between the light polarization vector and the plane of incidence. Note that Δn_2 and hence η_2 depend on the reading field E_R because of the function $f(E_R)$.

The gain coefficient

$$\Gamma = \frac{4\pi\Delta n_1 \sin\phi_g(K)}{m\lambda} = -\kappa\frac{4\pi n^3 g_{\text{eff}}}{\lambda}\epsilon_0^2\chi(E_W)\chi(E_R) \times \frac{1 + E_D/E_{qd} + E_W^2/\hat{\sigma}E_D E_{qe}}{(1+E_D/E_{qd})^2 + (E_W/E_{qe})^2}\hat{\sigma}E_D E_R \tag{18}$$

does not depend on the two-beam modulation degree m, but on κ.

We want to stress here that direct measurement methods for the stationary phase shift $\phi_g(K)$ are highly desirable, because $\phi_g(K)$ depends neither on m nor on κ [Eq. (14)] and hence not on quantities which depend on their turn on the y coordinate. While η_1 is reduced by κ and m as well, the gain coefficient Γ depends on κ(!) but not on m. This means e.g., that materials where the photoconductivity is a sublinear function of the intensity exhibit a lower diffraction efficiency and gain than would be expected for materials with linear photoconductivity. Furthermore, diffraction efficiency and gain will depend on intensity, if there is appreciable dark conductivity be-

cause of the factor $(1+\sigma_d/\sigma_{ph})^{-1}$. A further decrease of η_1 and Γ is to be expected for pronounced light scattering because of the factor $(1+I_s/I_0)^{-1}$. We are aware of the fact that we have not taken seriously into account the dependence on the y coordinate in a dynamic calculation. This turns out to be quite difficult for the special case of PLZT 10:65:35 and will remain as a future task. In the present investigation we want to show that without this refinement the above theory agrees already qualitatively with the experiment and quantitatively gives the correct orders of magnitude. The quantities m and κ have then in the following more the meaning of averages over the y coordinate or effective quantities.

III. THE EXPERIMENTAL METHOD

The PLZT 10:65:35 samples were produced from the chemically coprecipitated raw material by hot pressing in vacuum with a following extended annealing in ambient atmosphere. The samples are optically isotropic in the absence of an applied field. The thickness of the samples investigated ranges from 0.5 to 2 mm.

A detailed description of the holographic measurement equipment and data on the extinction, the electric polarization as a function of the electric field, and the electrooptic coefficients of the PLZT 10:65:35 samples are already published in Ref. 21. So we restrict ourselves to a few remarks concerning some differences between the earlier and the present investigation.

A grating with spacing $\Lambda=2.7$ μm is recorded by two beams of equal intensity I_{10} and I_{-10} with light wavelength $\lambda=488$ nm. The beam diameter is larger than the distance between the electrodes in order to illuminate the sample homogeneously. After termination of the recording process the phase shift ϕ_g is registered by two methods, which give analogous results. In the first one the sample, which is mounted on a translation table, is shifted along the z coordinate by means of a piezoelectric transducer (Fig. 1).[31] This imposes an external phase shift ψ which is 2π, if the crystal is displaced by $\Lambda=2.7$ μm. The transmitted intensities I_{+1} and I_{-1} change thereby sinusoidally according to

$$I_{\pm 1}-I_{\mp 1}\approx\pm\sin(\psi+\phi_g)\ . \tag{19}$$

The second method for the determination of ϕ_g is the microphotometric method described already elsewhere.[28,32] The diffraction efficiency η is calculated according to

$$\eta=\frac{\text{diffracted intensity}}{\text{diffracted intensity}+\text{transmitted intensity}}\ .$$

The notations η_1 and η_2 refer to θ_1 and θ_2, and η_{+1} and η_{-1} is used instead of η_1 if we want to differentiate between the intensities I_{+1} and I_{-1} diffracted while shutters block the beam intensities I_{+10} and I_{-10}, respectively.

The process of stationary energy transfer is characterized by the exponential gain factor

$$\Gamma=\frac{1}{d}\ln\left[\frac{I_{+1}I_{+10}}{I_{-10}I_{-1}}\right]\ .$$

Some of the experiments require the application of an electric voltage to the sample. In case of the measurements shown in Figs. 2–4 the planar electrode configuration shown in Fig. 3(a) has been used. The lines of equal electric potential are also plotted in Fig. 3(a) and demonstrate that the electric field is homogeneous over the gap range. But as pointed out already[33] the electric field is smaller than for end face electrodes. While for end face electrodes a voltage of 1 kV across the gap of 1 mm would produce a field of 10×10^5 V m^{-1} we have taken into account that only a reduced field of 8.3×10^5 V m^{-1} results for our planar electrodes.

IV. THE PHASE MISMATCH $\phi_g(K)$ AND THE PARAMETERS $\hat{\sigma}$, E_{qe}, AND E_{qd}

At first glance it seems to be natural to start holographic investigations of a refractive index grating with the determination of the diffraction efficiency. But a short inspection of the Eqs. (13), (16), and (17) should tell us that it will be quite frustrating to extract any useful information (e.g., $\hat{\sigma}$, E_{qe}, and E_{qd}) from the efficiency measurements by themselves. One reason is that we need g_{eff}

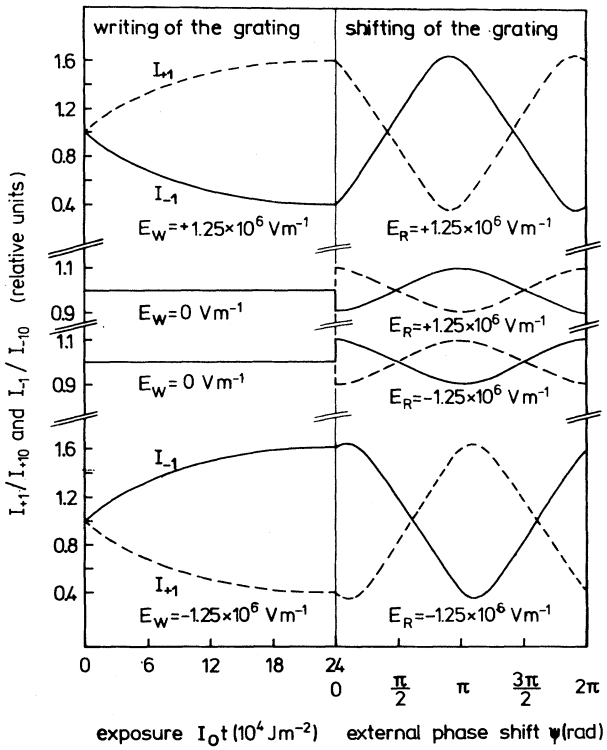

FIG. 2. Four exemplary experiments ($\lambda=488$ nm, $\Lambda=2.7$ μm) which show the change of transmitted intensities of the recording beams I_1 and I_{-1} during the recording process with applied electric field E_W and during the phase shift experiment with an external phase shift ψ and applied electric field E_R. The phase shift for the large electric field of 1.25×10^6 V m^{-1} approaches $\pi/2$.

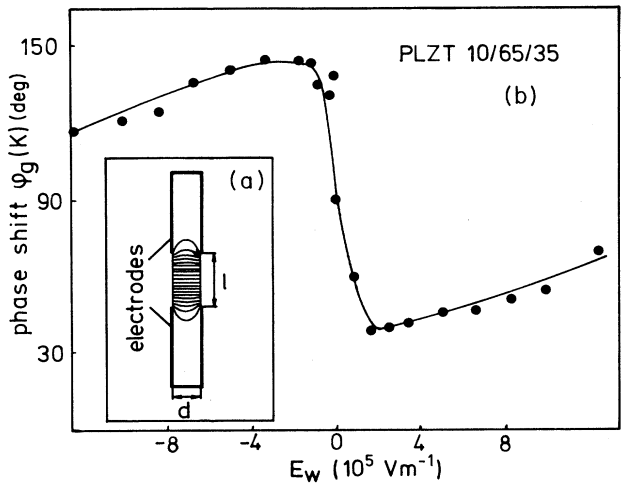

FIG. 3. (a) Geometric dimensions and distribution of equipotential lines of the sample used for the measurement shown in Figs. 2–4. Sample thickness is $d=0.5$ mm and gap between the electrodes is $l=1.0$ mm. (b) Experimental dependences of the phase mismatch between the holographic grating and the fringe pattern on the electric writing field ($\lambda=488$ nm, $\Lambda=2.7$ μm).

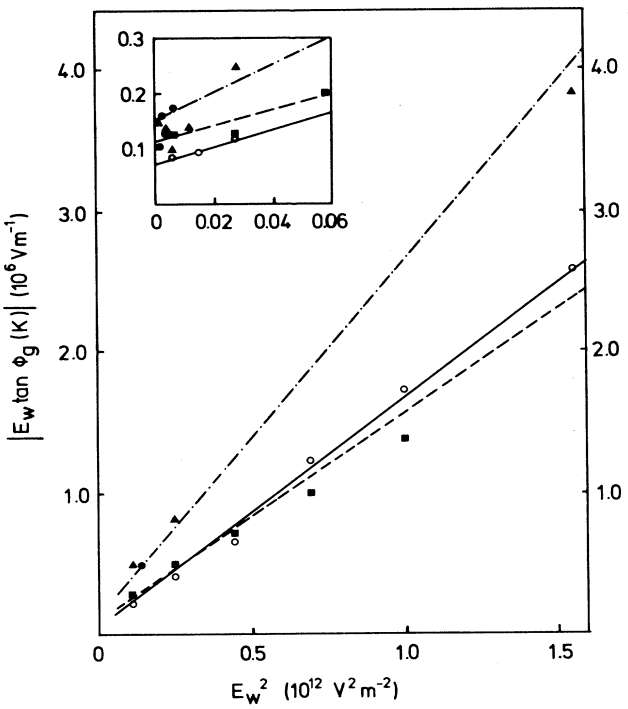

FIG. 4. $E_W\tan\phi_g$ is plotted as a function of E_W^2. The data were collected by four different experimental runs (▲, ●, ■, and ○, $\lambda=488$ nm, $\Lambda=2.7$ μm, room temperature). For three of them the field was applied in positive and for one in negative direction. The insert shows a magnified plot for $E_W\to 0$ in order to determine the intercept term. The limiting space charge field $E_q\approx 5\times 10^5$ V m^{-1} is estimated from the slope and $\hat{\sigma}E_D\approx 1\times 10^5$ V m^{-1} from the intercept term. The diffusion field is 0.6×10^5 V m^{-1}.

and the nonlinear relationship $P(E)$ for the calculation of Δn from the diffraction data. The main problem in PLZT 10:65:35, however, is the unknown parameters κ. Because of depolarization by ordinary scattering and strong light-induced scattering[34] κ decays along the y direction.[32] Additionally, the conductivity is not proportional to the light intensity. For PLZT 10:65:35 $\sigma_{\rm ph}\propto I^{1/2}$ and hence $x=\frac{1}{2}$ has been observed.[26] The value seems to depend somewhat on external parameters and the sample preparation. As it is rather difficult to estimate *ab initio* the effective value for κm correctly, we study the phase mismatch ϕ_g as a function of the externally applied writing field E_W first and evaluate Eq. (14).

For this purpose several gratings are written with the same grating spacing, wavelength, recording time ($t=10$ min) and with an exposure sufficient to reach the stationary state ($\approx 2.4\times 10^5$ J m^{-2}), but with an externally applied voltage varying from 0 to 2.0 kV which corresponds to fields up to 1.7×10^6 V m^{-1}.

When the recording experiment is finished, always the same voltage (1.5 kV) is applied for reading (This is only a cosmetic provision, because we utilize direct methods to determine the phase shift. The refractive index change must only be large enough for detection.) The intensity difference between the two coupling beams at the end of the recording and at the beginning of our shifting experiment is proportional to $\sin\phi_g(K)$ and will be denoted by $\Delta I(\phi_g)$. Subsequently the grating is shifted with respect to the standing light interference pattern. Because of beam coupling the intensities of the transmitted beams change sinusoidally as a function of the external phase shift ψ according to Eq. (19). From the record we determine the maximum intensity difference $\Delta I(\pi/2)$. It is denoted $\Delta I(\pi/2)$ because it corresponds to a total phase shift $\psi+\phi_g(K)=\pi/2$. Then $\tan\phi_g(K)=c/(1-c^2)^{1/2}$ is calculated from the ratio $c=\Delta I(\phi_g)/\Delta I(\pi/2)$. A representative experimental run is shown in Fig. 2. For $E_W=0$ only the diffusion mechanism contributes to the holographic recording process and $\phi_g(K)\approx\pi/2$ is observed. For small external electric fields $E_W<2.5\times 10^5$ V m^{-1} the phase mismatch decreases, passes a minimum at $E_W\approx 2.5\times 10^5$ V m^{-1} and increases again approaching asymptotically $\phi_g(K)=\pi/2$ for large electric fields [Fig. 3(b)]. The occurrence of a minimum is corroborated by several experimental runs.

Values obtained in four experimental runs, three with an applied field in positive and one in negative direction, are comprised in Fig. 4, where $|E_W\tan\phi_g(K)|$ is plotted as a function of E_W^2. From Eq. (14) we have

$$E_W\tan\phi_g(K)=a+bE_W^2\ , \tag{20}$$

where $a=E_D\hat{\sigma}(1+E_D/E_{qd})/(1+E_D/E_{qd}-\hat{\sigma}E_D/E_{qe})$ and $b=[E_{qe}(1+E_D/E_{qd}-\hat{\sigma}E_D/E_{qe})]^{-1}$. Using $E_D=0.6\times 10^5$ V m^{-1} for $\Lambda=2.7$ μm we calculate the conductivity factor $|\hat{\sigma}|=(\sqrt{1+4ab}-1)/2bE_D>0.9$ from the intercept term $|a|\approx(1.1\pm 0.5)\times 10^5$ V m^{-1} and the slope $b\approx(1.8\pm 0.5)\times 10^{-6}$ m V^{-1}. It was not possible to determine $\hat{\sigma}$ more accurately because of the bad reproducibility of different runs and because of the fact that we do not obtain the same curve for positive and

negative applied voltage [Fig. 3(b)]. One reason for the scattering of the measurement values may be that phase shift measurements are very sensible to vibration during recording. Some systematic deviations are also expected because E_{qd} and E_{qe} are not exactly constant but depend via $\epsilon(E_W)$ on E_W. But this can be neglected in view of our measurement accuracy. Because we know that the upper limit of $|\hat{\sigma}|$ is 1, we can restrict the values of $|a|$ further to be within the limit 0.6×10^5 V m^{-1} $\leq|a|\leq 0.7\times10^5$ V m^{-1}. As we find that $|\hat{\sigma}|$ is close to 1, we see in contrast to former results[8,19] no conclusive experimental evidence for compensated bipolar photoconductivity in PLZT 10:65:35 at $\lambda=488$ nm. If we put $\hat{\sigma}=1$ or $\hat{\sigma}=-1$, it follows from the Eqs. (10a) and (10b) that $E_{qd}=E_q$ and $E_{qe}=\hat{\sigma}E_q$, where $E_q=eN_{\text{eff}}/K\epsilon(E_W)\epsilon_0$ denotes the maximum space charge amplitude for dominating n-type or p-type conductivity and N_{eff} is the effective density N_n or N_p, respectively, of photoactive centers of the majority carriers. Then we get the following ranges: 2×10^5 V m$^{-1}\leq E_q\leq 8\times10^5$ V m^{-1}, 1×10^{23} m$^{-3}\leq N_{\text{eff}}\leq 5\times10^{23}$ m^{-3}, and 0.7 μm $\leq l_D\leq 1.5$ μm for the Debeye screening length. For the calculation we have used the value $\epsilon(E_W=5\times10^5$ V m$^{-1})$ $\approx 6\times10^3$.[21] Theoretical plots of ϕ_g as a function of E_W for $\hat{\sigma}=1$ and $E_{qe}\approx E_{qd}\approx E_q$ according to Eq. (14) are shown in Ref. 35.

V. DIFFRACTION EFFICIENCY AND MODULATION DEGREE DURING WRITING

The diffraction efficiencies η_{+1} and η_{-1} at the first-order Bragg angle θ_1 are measured with light polarization parallel to the reading field for a 1.9 mm thick sample with end face electrodes. In general a difference is observed which increases with long exposure and large writing fields E_W (Fig. 5). According to our observation this phenomenon goes along with increasing holographic scattering.[34] For negative applied field η_{-1} becomes larger than η_{+1} and for positive applied field it is vice versa. If the sample is shifted during writing not only the intensities of the two writing beams but also the scattered light become periodically modulated with the external phase shift.

In the following sections we identify the average diffraction efficiency $(\eta_{+1}+\eta_{-1})/2$ with η_1 and use it in order to calculate Δn_1 via Eq. (16). The curves $\eta_{+1}(I_0t)$ and $\eta_{-1}(I_0t)$ are symmetrical with respect to $\eta_1(I_0t)$. Frankly speaking we have at the moment no other reasons to do so but the fact that our procedure suggests itself, is correct for small fields, where $\eta_{+1}=\eta_{-1}$, and the results are reasonable. For smaller fields than in the extreme case shown in Fig. 5 the difference is nevertheless small and the problem not very crucial.

The interference pattern observed at the exit face of the sample becomes more and more deteriorated with exposure at constant field 1.0×10^6 V m^{-1} [Fig. 6(a)] or with increasing electric field at constant exposure $I_0t=2.4\times10^5$ J m^{-2} [Fig. 6(b)]. This is substantiated by microphotometric measurements[32] of the modulation degree m at the exit face of the sample (called contrast in Ref. 32). A typical result for $\Lambda=3$ μm and $E_W=1.0\times10^6$ V m^{-1} is shown in Fig. 6(c) as a function of exposure.

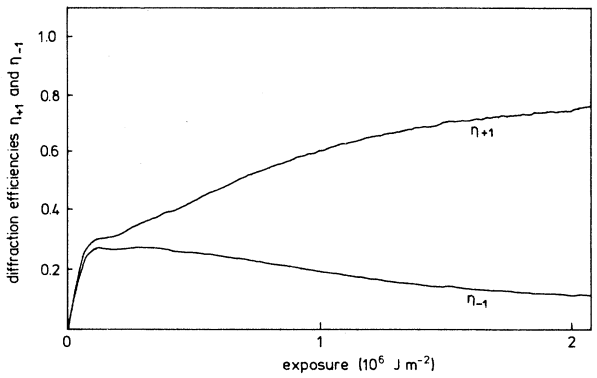

FIG. 5. The diffraction efficiencies η_{+1} and η_{-1} as a function of exposure for $E_W=1.0\times10^6$ V m^{-1}. The diffraction efficiency reaches very quickly an intermediate saturation value and splits then into an increasing and a decreasing branch. The average value $\eta_1=(\eta_{+1}+\eta_{-1})/2$ changes only very slowly for $I_0t>1\times10^5$ J m^{-2} in comparison to the quick initial rise.

VI. SATURATION DIFFRACTION EFFICIENCY AND ELECTRIC READING FIELD

After writing a refractive index grating with $\Lambda=3.0$ μm and an exposure $I_0t=2\times10^5$ J m^{-2} (approximately steady state) the diffraction efficiencies η_1 and η_2 are measured at the first and second order Bragg angle as a function of the reading field. Thereby the reading beam is incident in direction of the applied electric field and E_R is

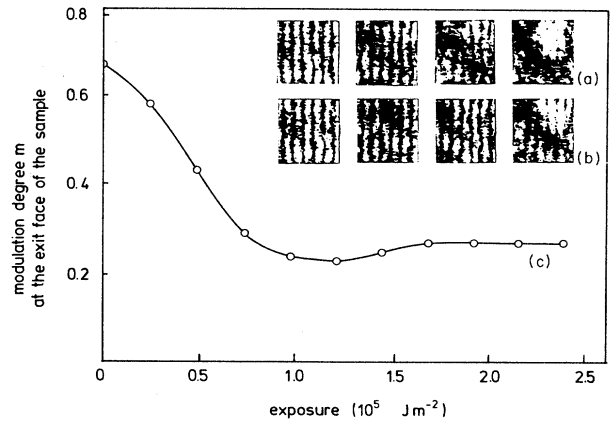

FIG. 6. (a) and (b) Microphotographs of the light intensity distribution at the exit face of the sample ($d=1.9$ mm). (c) Modulation degree at the exit face of the sample as a function of exposure. (a) From left to right: Exposure $I_0t=0$, 1.2×10^4, 7.2×10^4, and 3.6×10^5 J m^{-2}, electric field $E_W=-1.0\times10^6$ V m^{-1}, $\Lambda=2.7$ μm. (b) From left to right: Electric field $E_W=0$, -0.5, -0.75, and -1.0×10^6 V m^{-1}, exposure 2.4×10^5 J m^{-2}, $\Lambda=2.7$ μm. (c) $\Lambda=3.0$ μm, $E_W=1\times10^6$ V m^{-1}.

applied only for a short time compared to the writing time. The light polarization is parallel to the electric field. The refractive index amplitudes are calculated according to Eq. (16). This means that the information about the signs are lost and we get only $|\Delta n_1|$ and $|\Delta n_2|$. Our theory predicts [Eqs. (17a) and (17b)] the following:

(1) Not only Δn_1 but also Δn_2 depends on the electric reading field E_R.

(2) $|\Delta n_1|$ is a symmetrical function with respect to $E_R=0$ (long-known result[15]).

(3) $|\Delta n_2|$ is an asymmetrical function with respect to $E_R=0$ (demonstrated and explained here for the first time).

(4) The first-order refractive index amplitude

$$\Delta n_1(P_R)=\gamma P_R, \quad \text{with } \gamma=n^3 g_{\text{eff}} P_{\text{SC}}(K) \tag{21}$$

is proportional to the polarization induced by the reading field.

(5) For the second-order refractive index amplitude we have

$$\Delta n_2(P_R=0)=\tfrac{1}{4}\gamma_{P_{\text{SC}}}(K) . \tag{22}$$

(6) The minimum of Δn_2 occurs for an applied reading field of

$$E_{R,\min}=-\frac{1}{2}\frac{\zeta_3}{\zeta_1}\frac{1+(\hat{\sigma}E_D/E_W)^2}{1+(\zeta_2\hat{\sigma}E_D/\zeta_1 E_W)^2}E_W \tag{23}$$

and the refractive index amplitude at the minimum is given by

$$\Delta n_2(E_{R,\min})=\Delta n_2(E_R=0)\frac{\zeta_2\hat{\sigma}E_D/\zeta_1 E_W}{\sqrt{1+(\zeta_2\hat{\sigma}E_D/\zeta_1 E_W)^2}} . \tag{24}$$

The refractive index amplitudes $|\Delta n_1|$ and $|\Delta n_2|$ are shown in Figs. 7 and 8, respectively. The predictions

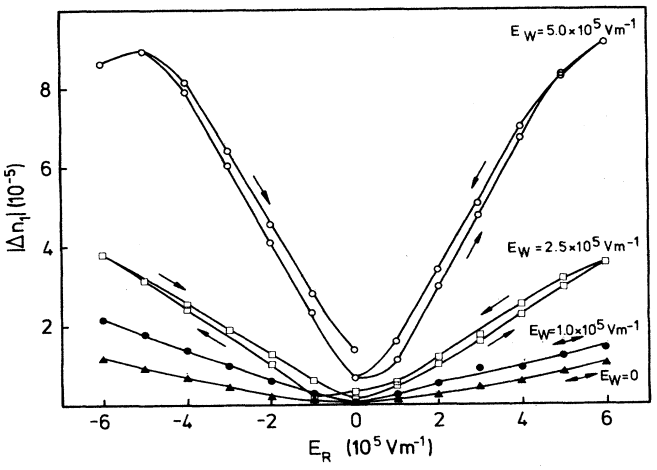

FIG. 7. The refractive index amplitude $|\Delta n_1|$ is a symmetrical function of the electric reading field E_R. The different writing fields applied are given in the figure and arrows indicate how the electric field was increased and decreased.

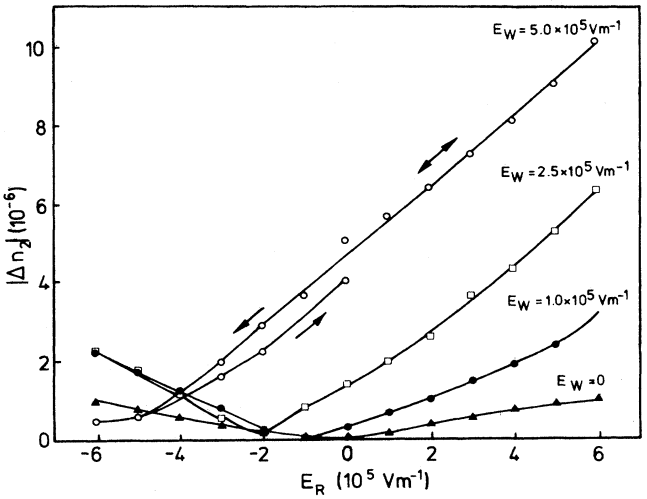

FIG. 8. The refractive index amplitude $|\Delta n_2|$ is an asymmetrical function of the electric reading field E_R. The different writing fields applied are given in the figure and arrows indicate how the electric field was increased and decreased. The position and heights of the minimum shifts with increasing writing field.

(1)–(3) are evidently correct.

The statements (4) and (5) can be drawn upon to determine in principle the absolute values of the space charge polarization,

$$P_{\text{SC}}(K)=4P_R\Delta n_2(0)/\Delta n_1(P_R) , \tag{25}$$

the effective electrooptic coefficient,

$$g_{\text{eff}}=4\Delta n_2(0)/n^3(P_{\text{SC}}(K))^2 , \tag{26}$$

with no further input data than the relationship between P and E besides the determination of the value $\Delta n_1(P_R)$ for any arbitrary applied electric field E_R and $\Delta n_2(E_R=0)$ by holographic means. But also the P-E relationship can be obtained from Fig. 7, if the slope of $\Delta n_1(E_R)$ which is proportional to P_R is plotted versus E_R. Then only the dielectric constant $\epsilon(E_R=0)$ is necessary in order to determine the proportionality constant. Note that even the slim-loop behavior of the hysteresis curve of PLZT 10:65:35 including remanence is fairly well resolved by the slope in Fig. 7, if the writing field is chosen large enough. The simple but powerful method outlined above can be applied not only for PLZT 10:65:35 but for all photorefractive materials with quadratic electrooptic effect.

A. A new holographic method for absolute measurements of g_{eff}

Gratings are written holographically with an exposure of 4.8×10^5 J m^{-2} and with an electric writing field $E_W=\pm5\times10^5$ V m^{-1} applied to a 1.9 mm thick sample. Reading out at the first order Bragg angle with the same reading field $E_R=E_W$ yields $\eta_1(E_R)=0.21$, while the diffraction efficiency at the second order transition is

determined with $E_R=0$ yielding $\eta_2(0)=2.1\times10^{-4}$. In both cases $\phi=0$, i.e., a light polarization parallel to the applied field has been chosen. With the help of Eqs. (16) and (25) we obtain from these values $P_{SC}/P_R=0.12$. From the results of Ref. 21 we have $P_R\approx0.027$ C m^{-2}. Then via Eq. (26) the effective electrooptic coefficient $g_{eff}=0.026\pm0.002$ m^{4}C^{-2} is calculated. The electrooptic coefficient is in agreement with the value obtained by the conventional polarization optic method.[21]

B. Minima of $\Delta n_2(E_R)$ and their relation to characteristic material parameters

Using $E_D=0.6\times10^5$ V m^{-1} and $E_q=5\times10^5$ V m^{-1} we calculate with the help of Eq. (23) for $E_W=1$, 2.5, and 5×10^5 V m^{-1} that minima should occur for $E_{R,\min}=-1.1$, -2.6, and -5.1×10^5 V m^{-1}. Experimentally we find $E_{R,\min}=-1$, -2, and -6×10^5 V m^{-1}. The comparison is quite satisfactory and corroborates again that the maximum space charge field E_q is in the scope of our applied electric field for our PLZT 10:65:35 samples (e.g., for $E_q\gg E_D,E_W$ the result would be $E_{R,\min}=-\frac{1}{2}E_R$). In principle $|\hat{\sigma}|$ can be determined from the ratio of the refractive index amplitudes $\Delta n_2(E_{R,\min})/\Delta n_2(E_R=0)$ (though it is not possible to distinguish by measurements of $\Delta n_2(E_{R,\min})$ between electrons and holes, because of $E_{qe}\propto\hat{\sigma}$ for $\hat{\sigma}=\pm1$). However, the measurements are not correct, possibly because of erasure during read-out and because of a hysteretic behavior at larger electric fields.

C. Impact of polar microregions on the first-order diffraction efficiency

If the grating is written with large writing fields (this refers e.g., to the curve for $E_W=5\times10^5$ V m^{-1} in Fig. 7), then there is no reading field where $\Delta n_1(E_R)$ becomes zero. Especially the observed remanent diffraction for $E_R=0$ is not predicted by the theory outlined above. If we examine the light distribution across the diffracted beam profile, we find a granular, inhomogeneous pattern for $E_R=0$, while the beam profile is as expected homogeneous as long as E_R is different from zero and large enough. If the sample is heated, the remanent diffraction disappears, but reappears when the sample is cooling again to room temperature. There is only a small efficiency loss by this procedure so that several heating-cooling cycles can be performed before the diffracted beam becomes too weak to be observed. In opposition to this, gratings erased with incoherent light can no more be recovered.

From the ratio of the diffraction efficiencies arcsin $(\eta_{1\parallel}^{1/2})/\arcsin(\eta_{1\perp}^{1/2})$ for polarization parallel and perpendicular to the reading field the ratio $g_{33}/g_{13}\approx2$ is measured for $E_R\to0$ and $g_{33}/g_{13}\approx7$ for large applied fields.

VII. SATURATION DIFFRACTION EFFICIENCY AS A FUNCTION OF THE ELECTRIC WRITING FIELD

The diffraction efficiency η_1 at saturation is investigated as a function of the writing fields E_W, while the reading field is kept constant at $E_R=1.0\times10^6$ V m^{-1}. The refractive index amplitude Δn_1 calculated via Eq. (16) from the experimental data is shown in Fig. 9 for different grating spacings Λ. Two features are remarkable: Firstly, there is a striking dependence on the grating spacing even in a range, where the writing fields largely surpass the diffusion field. Secondly, the relationship $\Delta n_1(E_W)$ has a maximum and Δn_1 becomes smaller again if electric writing fields larger than 7.5×10^5 V m^{-1} are applied.

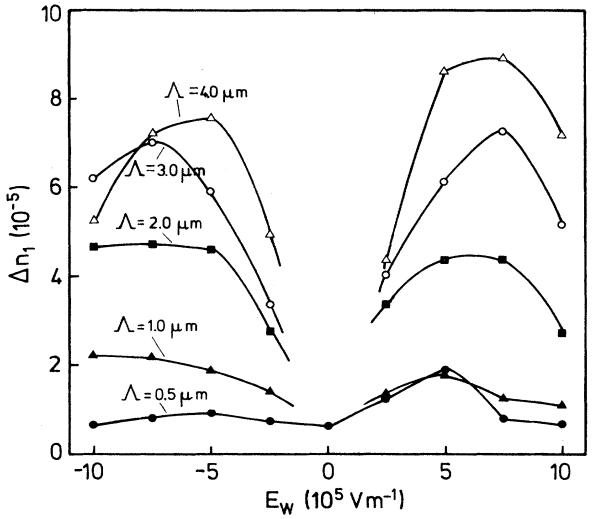

FIG. 9. The refractive index amplitude $|\Delta n_1|$ vs the electric writing field E_W for different grating spacings Λ and constant reading field $E_R=1.0\times10^6$ V m^{-1}.

VIII. HOLOGRAPHIC GAIN

For fields larger than 2×10^5 V m^{-1} the gain depends nearly linearly on the external electric field and rises with increasing grating spacing (Fig. 10). Our results agree with the results of Butusov *et al.*,[8] if we take into account that the polarization electrooptic coefficient as well as the

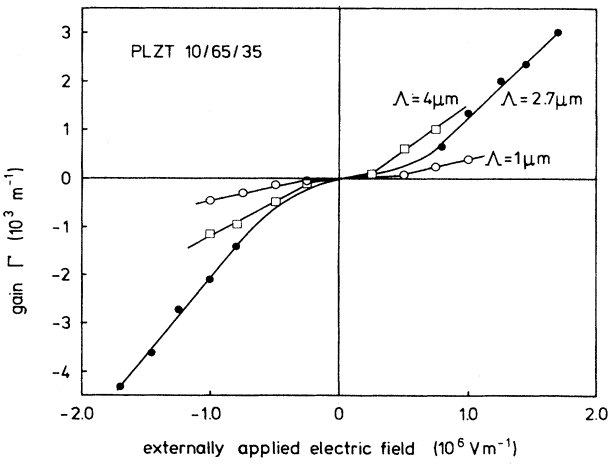

FIG. 10. Holographic gain Γ vs external electric field for different grating spacings ($\Lambda=488$ nm, $I_0t\approx2.4\times10^5$ J m^{-2}).

polarization which is induced by a given electric field at room temperature are larger for PLZT 9.2:65:35 than for PLZT 10:65:35. The electric field electrooptic coefficients are about 9 times larger[36] and this fits with the fact that Butusov *et al.* have observed for comparable grating spacings a gain which is about 10 times larger than our values.

IX. DISCUSSION

In Sec. IV we have demonstrated by phase shift measurements that there is no need for the assumption of a compensated bipolar conductivity. Now we will put forward some additional arguments.

The slopes of Fig. 7 are proportional to $P_{SC}(K)$. We divide the ratio of the slopes for writing with an applied field by the slope for $E_W=0$. For the small fields applied we can disregard the small nonlinearity of the P-E relationship, i.e., the factor $\kappa m \epsilon_0 \chi(E_W)$ of Eq. (15) drops out and we calculate for the values $\hat{\sigma}=1$ and $E_q=3\times10^5$ V m^{-1} determined in Sec. IV the ratios 5.4, 3.9, and 2.0 via Eq. (15). Experimentally we find 7.1, 2.4, and 1.4. Because on the one hand writing with electric fields is practically not affected by compensated bipolar conductivity, but on the other hand $P_{SC}(K)\propto \hat{\sigma}E_D/(1+E_D/E_q)$ should be smaller than $E_D=Kk_BT/e$ for $E_W=0$, we see again that apart from a possible factor 0.5 (which is only admitted because of our bad measurement accuracy) there is no room for the assumption of a nearly compensated bipolar conductivity. According to Eq. (22) the same ratios 5.4:3.9:2.0:1 are also expected for $\sqrt{\Delta n_2(0)}\propto P_{SC}(K)$. Experimentally we find the ratios 7.1:3.7:1.7:x. Unfortunately the ratio x for diffusion writing could not be determined, because the diffracted intensity was too small. The agreement of the results of quite different experimental runs, namely phase shift measurements, diffraction efficiency measurements at the first Bragg angle as a function of the reading field, and measurements at the second-order Bragg angle with the theoretical calculation gives us some confidence in our statement that the conductivity is nearly monopolar though we are aware of the fact that this is at variance with Refs. 8 and 19.

Low values for E_q limit the holographic resolution. This can be best understood in terms of the electric modulation transfer function

$$G(K)=\frac{P_{SC}(K)}{P_{SC}(0)}=\frac{\left\{\left[E_W+E_W\frac{E_D}{E_{qd}}-E_W\hat{\sigma}\frac{E_D}{E_{qe}}\right]^2+\left[\hat{\sigma}E_D+\hat{\sigma}\frac{E_D^2}{E_{qd}}+\frac{E_W^2}{E_{qe}}\right]^2\right\}^{1/2}}{[(1+E_D/E_{qd})^2+(E_W/E_{qe})^2][E_W^2+(\hat{\sigma}E_D)^2]^{1/2}}, \tag{27}$$

which is plotted in Fig. 11 as a function of the normalized spatial frequency K/K_D for $|\hat{\sigma}|=1$ [$G(K)$ does not differ for $\hat{\sigma}=+1$ and $\hat{\sigma}=-1$]. Here we introduce the cutoff frequency $K_D=2\pi/l_D$, where l_D is the Debeye screening length which is about 1.4 μm in our case. We take the calculated values G for 4 μm as reference and normalize all measurements shown in Fig. 9 by $G(4\ \mu\text{m})\Delta n_1(\Lambda)/\{\Delta n_1(4\ \mu\text{m})[1+(E_D/E_W)^2]^{1/2}\}$. The normalized measurement points are also shown in Fig. 11 and are in excellent agreement with the transfer function for $l_D=1.4$ μm and all electric fields applied. It is very instructive to try tentatively $l_D=0.7$ μm or 2.8 μm, because the measurement points will not fit at all. This proves that the holographic resolution expressed by the transfer function G and hence also the diffraction efficiency of PLZT 10:65:35 are dramatically reduced by the large Debeye screening length. The origin is the large dielectric constant which even increases, if electric fields are applied (cf. 21). The available donor (acceptor) density is too small to equibalance this resolution limiting effect. As a consequence, the material is—at least in the present quality— unsuitable for holographic recording applications where high resolution requirements are necessary. With that the first of the two remarkable features mentioned in Sec. VII is explained.

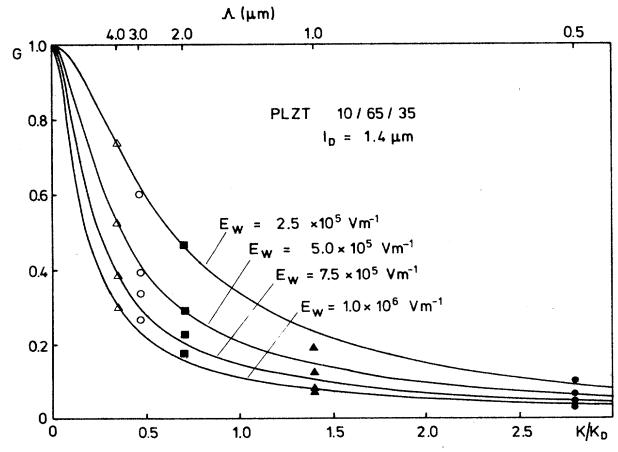

FIG. 11. Electric modulation transfer function G as a function of the normalized spatial frequency K/K_D. The cutoff frequency is small for large screening length $l_D\approx1.4$ μm. The measurement points of Fig. 9 normalized to the data for 4 μm are also plotted.

We will show now that the qualitative behavior of the gain is well described by the dynamic holographic theory and that a satisfactory quantitative agreement is achieved, if we assume that $\kappa<1$: With the parameters $\kappa=0.13$, $n=2.58$, $g_{\text{eff}}=0.026$ m^4 C^{-2},[21] $\epsilon_0=8.9\times10^{-12}$ C V^{-1} m^{-1}, $\chi(E)=5.5\times10^3+(2.5\times10^{-9}$ m^2 V$^{-2})E^2-(1\times10^{21}$ m^4 V$^{-4})E^4$,[21] $l_D=1.4$ μm, and $\hat{\sigma}=1$ the gain Γ has been calculated as a function of the externally applied electric field $E_{ex}=E_W=E_R$ using Eq. (18). The result is plotted in Fig. 12 together with the measurement points of Fig. 10. We have not extended our comparison

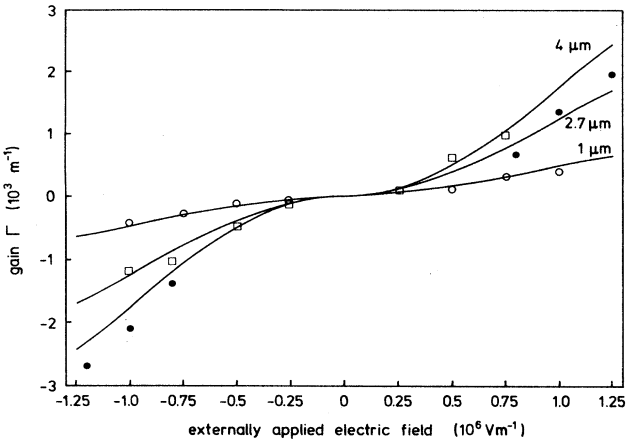

FIG. 12. Measured values of the gain and curves calculated with $\kappa=0.13$ and other parameters given in the text as a function of the electric field $E_{ex}=E_W=E_R$.

beyond $E_{ex}=1.25\times10^6$ V m^{-1}, because the approximation for the relationship $\chi(E)$ is only valid for electric fields up to 1.1×10^6 V m^{-1} (Ref. 21). The theoretical curves fit the measurements satisfactorily for positive applied fields and for $\Lambda=1$ μm over the whole range investigated. There are essentially three possibilities why κ can be smaller than 1: large dark conductivity, nonlinear photoconductivity, and large light scattering. As we have not observed a marked intensity dependence of the diffraction efficiency, we think that the contribution due to dark conductivity is small. If we take into account the exponent of the nonlinear photoconductivity by $x=0.5$, there remains still a factor of 0.26 which must be attributed to light scattering and depolarization during the writing process (as e.g., observed for holographic writing in $LiNbO_3$.[32] Indeed it has been shown that there is already an appreciable initial scattering and depolarization at the beginning of the writing process for PLZT 10:65:35 under an applied electric field.[34] As the scattering increases with the electric field, this would not be at variance with the second of the remarkable features mentioned in Sec. VII, namely the fact that the refractive index amplitude decays for large electric fields again.

We calculate now via Eqs. (13) and (17a) the factor κm. Thereby we use except for κ the same input parameters as above. The data are shown in Table III as a function of E_W and Λ. Note the very homogeneous distribution about the average value $\kappa m=0.26\pm0.07$ (relative deviation is about 30%). We find $\kappa m=0.19$ for $E_W=0$, which is not too different from the values obtained with an applied field $E_W\neq0$. This is obviously in favor with the assumption that for our sample and $\lambda=488$ nm there is no prevailing compensation by the bipolar conductivity. Even if we assume $m=1$, the value $\kappa\approx0.26$ obtained from diffraction efficiency data is twice as large than the value $\kappa\approx0.13$ obtained from the gain measurements. A possible explanation for this discrepancy is that Eq. (18) accounts for dynamic effects during writing, while Eq. (16) does not. Usually the diffraction efficiencies calculated according to Eq. (16) and calculated according to dynamic theory make not a large difference. But as we found for large electric fields $\phi_g\rightarrow\pi/2$ in PLZT 10:65:35 and hence large energy transfer, the light intensity modulation is not constant but decays in y direction.[32] This suggests that the diffraction efficiency of the dynamic theory seems to be more adequate than Eq. (16) and would be another interesting consequence of the low values for E_q.

The remanent diffraction efficiency of about 0.3% at $E_R=0$ observed in Fig. 7 cannot be explained for a homogeneous material with quadratic electrooptic effect. A possible remanent polarization P_R can be excluded as the origin of this remanent diffraction efficiency: Remanent polarization appears also, but only affects the slope of the $\Delta n_1(E_R)$ curve in accordance with Eq. (21). If the direction of E_R is changed and the small coercitive field is reached there is no doubt that P_R and hence $|\Delta n_1|$ must pass through zero. We think that an explanation should start with our observation that the beam profile of the remanently diffracted beam shows a granular structure. This structure reflects inhomogeneities of the material which are possibly due to ferroelectric regions stabilized by the high amplitude of the periodic space charge polarization. As regions which are in the quadratic phase do not diffract at $E_R=0$, we think, that holography is an extremely sensitive method to study the spatial distribution of such remanently poled regions in PLZT. Heating

TABLE III. The values κm calculated from the measurements shown in Fig. 9 for different grating spacings Λ and different writing fields E_W.

E_W (10^5 V m^{-1})	κm for $\Lambda=0.5$ μm	κm for $\Lambda=1.0$ μm	κm for $\Lambda=2.0$ μm	κm for $\Lambda=3.0$ μm	κm for $\Lambda=4.0$ μm
−10	0.14	0.25	0.27	0.24	0.16
−7.5	0.19	0.26	0.29	0.30	0.25
−5.0	0.27	0.26	0.33	0.30	0.32
−2.5	0.20	0.22	0.26	0.26	0.33
0	0.19				
+2.5	0.34	0.22	0.32	0.26	0.27
+5.0	0.49	0.23	0.32	0.31	0.36
+7.5	0.19	0.15	0.28	0.31	0.30
+10	0.16	0.13	0.16	0.20	0.22

the sample would induce a transition to the paraelectric state also for these regions, but they stabilize again on cooling. This concept is in accordance with our observations (Sec. VI C). The ratio $g_{33}:g_{13}$ depends sensitively on the structure of the material, too, and should be different for regions in the ferroelectric and paraelectric phase. In fact an appreciably lower ratio has been measured for the case where remanent diffraction at θ_1 prevails (Sec. VI C). With increasing electric fields the regions in the paraelectric phase can take part in the diffraction process via the quadratic electrooptic effect. Finally they will largely overcome the contribution of the ferroelectric regions. Another possibility for the different ratios are regions with clamped electrooptic effect.

Differing diffraction efficiencies $\eta_{+1} \neq \eta_{-1}$ have already been extensively studied and observed by Knyazkov and Lobanov.[37–40] One explanation given is the Borman effect.[37–39] This means that the planes of high light intensity of the interference pattern of the transmitted and diffracted beams coincide more or less with the maximum scattering planes depending on the direction of the incident beam. We doubt that the usual Borman effect will account for the large difference observed because the modulation of the absorption is too small in PLZT 10:65:35. More successful is a second model proposed by Knyazkov and Lobanov[40] which is based on the fact that holographic scattering is unidirectional in PLZT and hence breaks the symmetry of the diffraction efficiency at $\pm\theta_1$. If a direct influence of the oscillating intensities of the writing beams could be excluded, the observed energy transfer between writing beams and scattered beams with the external phase shift would fit the Knyazkov-Lobanov model.

X. CONCLUSIONS

Holographic resolution in PLZT 10:65:35 is limited by the available donor (acceptor) density and because of the large dielectric constant of the material. For holographic applications either further modifications (e.g., doping, oxidation/reduction treatments or a different ceramic processing) or an other composition with better properties (e.g., smaller ϵ) should be chosen. From the results of phase shift measurements $N_{\text{eff}} \approx 3 \times 10^{23}\ \text{m}^{-3}$ has been determined which corresponds to a Debye screening length of $l_D = 1.1\ \mu\text{m}$. A value $l_D = 1.4\ \mu\text{m}$, however, fits much better with diffraction efficiency measurements (Fig. 11). There is no indication on strongly compensated bipolar conductivity (i.e., $\hat{\sigma} \approx 1$).

The gain is also considerably reduced and becomes rapidly smaller with decreasing grating spacing (Fig. 10 and 12). But as the gain is proportional to $\chi^2 E_q \propto \chi^2/\epsilon$ the gain becomes larger if compositions are chosen, where the temperature T_m for the maximum dielectric constant is as close to room temperature as possible. As the maximum of the dielectric constant is related to the compositional broadening parameter δ,[21] it should be one task of the future development of ceramic technology to achieve a small broadening parameter δ. Furthermore, the holographic gain can be tailored to some extent by a proper choice of E_q, which may be interesting for image amplification.[41] It is obvious that for other photorefractive materials which are used close to the phase transition temperature and which have as a consequence a large ϵ (e.g., $\epsilon > 10\,000$ for KTN at room temperature and $BaTiO_3$ at 120° C) our comments apply correspondingly. We want to draw attention to the fact that holographic results for $BaTiO_3$ and other materials with a sublinear relationship $\sigma_{\text{ph}} \propto I^{\kappa}$ ($\kappa < 1$) are usually analyzed by theories which are based on a linear relationship, i.e., $\kappa = 1$, and hence a theory which is based on an essential wrong assumption. With our phenomenologic theory we can answer the question posed by Mullen,[42] if there is any influence of a nonlinear photoconductivity law on holographic results, in the following way: measurement techniques based on phase shift measurements are not affected by the nonlinear intensity dependence, but diffraction efficiency and gain measurements are. As the factor κ is presently disregarded in the analysis of the holographic results e.g., for $BaTiO_3$, results for Δn_1 and Γ come out by a factor κ lower than expected. In contrast, we cannot confirm the nonexponential decays during erasure reported by Mullen (Ref. 42, Fig. 6.8). We still simply think that $\Delta n = \arcsin(\sqrt{\eta})$ is proportional to $\exp(-t/\tau)$ and not η which makes a difference in the range $0 \leq \ln\eta \leq -1$.

Our experimental findings show that the close phase transition of PLZT 10:65:35 ceramics induces nonlinearities which influence the holographic properties. This favors a theoretical description in terms of electric polarization rather than in terms of electric fields. The description is qualitatively correct and quantitatively the disagreement is less than a factor of 2 even in the worst case. The spatial distribution of polar regions within the nonpolar phase can be studied by first order Bragg diffraction.

One of the disadvantages in PLZT 10:65:35 is holographic scattering.[34] From our experiments we draw the conclusion that the problem can be reduced by either writing with diffusion field only (reading with a large applied electric field and hence appreciable diffraction efficiencies for read-out are still possible) or by using light polarized perpendicularly to the field while an electric field is applied during writing (smaller electrooptic effect). In both cases we exploit the fact that writing is then essentially latent.

Second order diffraction is an efficient tool to obtain material parameters by holographic means. The most surprising is the possibility of absolute determination of electrooptic coefficients.

ACKNOWLEDGMENTS

We thank Dr. K. Betzler for the calculation of the equipotential lines of our sample [Fig. 3(a)]. Thereby the program described in Ref. 43 has been used. We thank Professor Dr. E. Krätzig for his encouragement and Professor A. Knyazkov and Dr. M. Lobanov for discussions. This work has been performed within the program of the SFB 225 "Oxide Crystals for Electro- and Magnetooptical Applications" financially supported by the Deutsche Forschungsgemeinschaft.

[1]P. Günter, Physics Reports **93**, 200 (1982).
[2]E. Krätzig and R. Orlowski, Appl. Phys. **15**, 133 (1978).
[3]A. Krumins and P. Günter, Appl. Phys. **19**, 153 (1979).
[4]J. P. Huignard, J. P. Herriau, G. Rivet, and P. Günter, Opt. Lett. **5**, 102 (1980).
[5]P. Günter, Opt. Lett. **7**, 10 (1982).
[6]A. E. Krumins, Ferroel. Lett. **1**, 89 (1983).
[7]A. E. Krumins, A. V. Knyazkov, A. S. Saikin, and I. A. Seglinsh, Sov. Phys. Solid State **25**, 908 (1983).
[8]M. M. Butusov, A. V. Knyazkov, A. S. Saikin, N. V. Kukhtarev, and A. E. Krumins, Ferroel. **45**, 63 (1982).
[9]N. V. Kukhtarev, V. L. Vinetsky, V. B. Markov, S. G. Odulov, and M. S. Soskin, Ferroel. **22**, 961 (1979).
[10]C. E. Land, Ferroel. **7**, 45 (1974).
[11]W. R. Bussem and T. I. Prokopowicz, Ferroel. **10**, 225 (1976).
[12]A. Kumada, G. Toda, and Y. Otomo, Ferroel. **7**, 367 (1974).
[13]J. M. Rouchon, M. Vergnolle, and F. Micheron, Ferroel. **11**, 389 (1976).
[14]J. W. Burgess, R. J. Hurditch, C. J. Kirkby, and G. E. Scrivener, Appl. Opt. **15**, 1550 (1976).
[15]B. Houlier and F. Micheron, J. Appl. Phys. **50**, 343 (1979).
[16]F. Micheron, C. Mayeux, and J. C. Trotier, Appl. Opt. **13**, 874 (1974).
[17]A. E. Krumins, E. E. Klotins, V. I. Dimza, U. Yu. Ilyin, and V. J. Fritsberg, Ferroel. **18**, 21 (1978).
[18]A. E. Krumins, U. Y. Ilyin, and V. I. Dimza, Ferroel. **22**, 695 (1978).
[19]A. E. Krumins, V. I. Dimza, J. J. Seglins, and A. A. Sprogis, Ferroel. **63**, 253 (1985).
[20]F. Micheron, J. M. Rouchon, and M. Vergnolle, Appl. Phys. Lett. **24**, 605 (1974).
[21]R. A. Rupp, K. J. Kerperin, and A. E. Krumins (unpublished).
[22]K. Uchino, M. Aizawa, and L. S. Nomura, Ferroel. **64**, 199 (1985).
[23]A. V. Knyazkov and M. N. Lobanov, Sov. Tech. Phys. Lett. **13**, 313 (1987).
[24]A. E. Krumins and V. Y. Fritsberg, Ferroel. **35**, 149 (1981).
[25]G. Schwitzgebel, J. Maier, and U. Wicke, Z. Phys. Chem. **130**, 97 (1982).
[26]A. E. Krumins and M. Vanecek, Phys. Stat. Sol. A **33**, K31 (1976).
[27]R. Orlowski and E. Krätzig, Solid State Commun. **27**, 1351 (1978).
[28]R. Matull and R. A. Rupp, J. Phys. D **21**, 1556 (1988).
[29]T. J. Hall, R. Jaura, L. M. Connors, and P. D. Foote, Prog. Quant. Electron. **10**, 77 (1985).
[30]S. F. Su and T. K. Gaylord, J. Opt. Soc. Am. **65**, 59 (1975).
[31]R. Orlowski and E. Krätzig, Ferroel. **26**, 841 (1980).
[32]R. A. Rupp, Appl. Phys. B **42**, 21 (1987).
[33]P. D. Thacher, J. Appl. Phys. **41**, 4790 (1970).
[34]A. Krumins, K. H. Ringhofer, R. A. Rupp, and F. Shi (to be published).
[35]A. Krumins, R. A. Rupp, and K. Kerperin, Ferroel. **80**, 281 (1988).
[36]G. H. Haertling and C. E. Land, J. Am. Ceram. Soc. **54**, 1 (1971).
[37]A. V. Alekseev-Popov, A. V. Knyazkov, and A. S. Saikin, Sov. Tech. Phys. Lett. **9**, 475 (1983).
[38]A. V. Knyazkov and M. N. Lobanov, Opt. Spectrosc. **59**, 770 (1985).
[39]A. V. Knyazkov and M. N. Lobanov, Pisma v JTP **11**, 882 (1985).
[40]A. V. Knyazkov and M. N. Lobanov, Opt. Spectrosc. **64**, 243 (1985).
[41]T. Tschudi, A. Herden, J. Golz, H. Klumb, F. Laeri, and J. Albers, IEEE J. Quant. Electron. **22**, 1493 (1986).
[42]R. A. Mullen, in *Photorefractive Materials and their Applications I,* Vol. 61 of *Topics in Applied Physics,* edited by P. Günter and J. P. Huignard (Springer-Verlag, Berlin, 1988), p. 167.
[43]K. Betzler, B. Hellermann, and H. Hesse, Ferroel. Lett. **7**, 143 (1987).
[44]W. A. Schulze, J. V. Biggers, and L. E. Cross, J. Amer. Ceram. Soc. **61**, 46 (1978).
[45]A. V. Shilnikov, A. I. Burkhanov, L. I. Dentsova, and E. G. Nadinskaya, Ferroel. **69**, 111 (1986).
[46]A. Corullon and B. Jimenez, Ferroel. **54**, 167 (1984).